Monte Carlo simulation and integral-equation studies of a fluid of charged hard spheres near the critical region

F. Bresme
Departamento de Química-Física, Facultad de Ciencias Químicas, Universidad Complutense de Madrid, E-28040 and Instituto Química-Física Rocasolano, Consejo Superior de Investigaciones Científicas, Serrano 119, E-28006 Madrid, Spain

E. Lomba
Instituto de Química-Física Rocasolano, Consejo Superior de Investigaciones Científicas, Serrano 119, E-28006 Madrid, Spain

J. J. Weis
Laboratoire de Physique Théorique et Hautes Energies, Bâtiment 211, Université de Paris-Sud, 91405 Orsay Cedex, France

J. L. F. Abascal
Departamento de Química-Física, Facultad de Ciencias Químicas, Universidad Complutense de Madrid, E-28040, Spain
(Received 18 April 1994; revised manuscript received 24 August 1994)

A detailed Monte Carlo and integral-equation study of the behavior of the restricted primitive model of electrolytes near the critical region is presented. Our simulation results furnish information concerning cluster formation in the low density–high ionic strength region. Additionally, bridge functions have been extracted from the simulated pair correlation functions by means of an iterative procedure. These "exact" bridge functions have been compared with the results of a recently proposed integral equation [D.M. Duh and A.D.J. Haymet, J. Chem. Phys. **97**, 7716 (1992)] which has been solved using both a Coulombic and an optimized decomposition of the interionic potential.

PACS number(s): 61.20.−p, 64.60.Fr, 64.70.Fx

I. INTRODUCTION

Recent debate on the critical behavior of ionic fluids [1] has given rise to renewed interest in the theoretical study of the restricted primitive model (RPM), the simplest system in which these questions can be investigated. In particular two independent Monte Carlo (MC) studies [2,3] have succeeded in establishing the gas-liquid coexistence curve and critical point with a high degree of confidence. An essential feature of the low density–low temperature ionic fluid is the strong tendency of the ions to associate into dipolar pairs, triplets, and higher order clusters [4,5], and any theory which aims at describing with some success its critical behavior will have to cope with this fact. A recent Debye-Hückel-Bjerrum type theory extended to allow for association of the ions into neutral dipolar pairs has indeed proven [6] to be able to give a reasonable representation of the simulated coexistence curve.

The purpose of this paper is to investigate the structural behavior of the RPM when approaching the critical temperature along an isochore of density approximately one-third of the critical density. Special emphasis is placed on the determination of the bridge functions from the simulation results. Recently, related works focused on nonionic systems [11,12], have been published. In fact, the bridge function is the necessary ingredient to improve integral equation theories, such as the hypernetted-chain (HNC) equation [7], extensions of the mean spherical approximation (MSA) MSA [8,9], or the crossover and hybrid MSA (HMSA) approximations [10], which perform poorly in the low density–high ionic strength region, where one should expect to find criticality.

The rest of the paper can be sketched as follows. Our most representative simulation results are presented in Sec. II. The integral-equation approach to the problem, as well as the iterative procedure for the extraction of the bridge functions from the simulation data, are discussed in Sec. III. Here we also compare the "exact" bridge functions with the results of a recently proposed integral equation [13], using both a Coulombic and an optimized decomposition of the interionic potential. Finally, our main conclusions are summarized in Sec. IV.

II. MONTE CARLO SIMULATIONS

A. Model potential and simulation details

The Monte Carlo simulations were performed in the canonical ensemble for a system of 512 positive and 512 negative ions in a cubic box with periodic boundary conditions. The particles interact through the potential,

$$u_{\alpha\beta}(r) = \begin{cases} \infty & \text{if } r < \sigma \\ \frac{Z_\alpha Z_\beta e^2}{\epsilon r} & \text{if } r \geq \sigma, \end{cases} \tag{2.1}$$

sum of a hard sphere (HS) repulsion and a long-range Coulomb term, defining the RPM model.

In Eq. (2.1), $Z_\alpha = \pm 1$ is the ionic charge, ϵ the dielectric constant of the solvent, e is the electron charge in esu, and σ the hard sphere diameter. The long-range Coulomb interactions were taken into account using Ewald's method [14]. The density of the system was $\rho^* = \rho\sigma^3 = 0.01$ and the inverse temperature $\beta^* = e^2/\epsilon kT$ was varied from 4 to 18. We recall that the best estimates of the critical parameters presently available for the RPM are $\beta_c^* \sim 18.9$ and $\rho_c^* \sim 0.025$ [2(b)] and $\beta_c^* \sim 17.5$ and $\rho_c^* \sim 0.04$ [3]. The sampling of configuration space was performed using the standard Metropolis algorithm, i.e., a particle trial move consisted of a random displacement inside a cube of edge 2δ centered at the old particle position. The value of δ was chosen to obtain an acceptance ratio of 0.45–0.50. Typical values range from $\delta = \sigma$ at the highest temperature to $\delta \approx 0.2\sigma$ at the lowest. With these values substantial diffusion of the ions was observed along the simulation runs, which involved between 20 000 and 48 000 trial moves per particle after equilibration of the system.

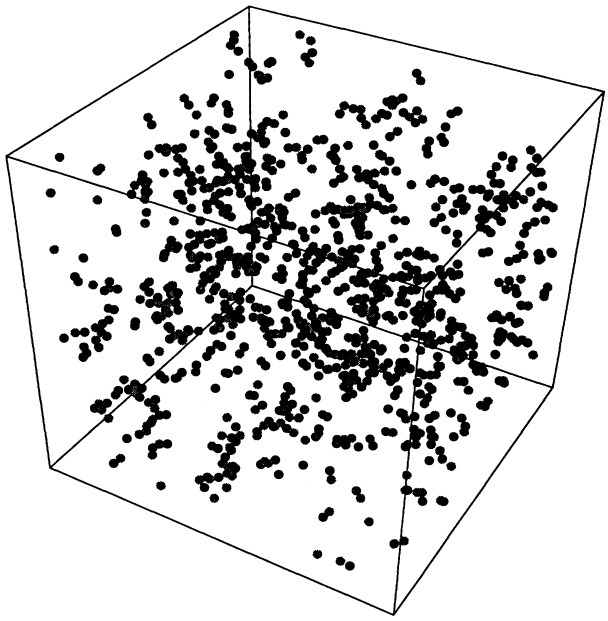

FIG. 2. Same as Fig. 1 but for $\beta^* = 10$.

B. Simulation results

Snapshots of configurations of the system are shown in Figs. 1–4 for $\beta^* = 4$, 10, 15, and 18. Whereas at $\beta^* = 4$ the system is fairly homogeneous, substantial clustering of the ions is visible at $\beta^* = 10$ and lower temperatures. Formation of two-, three-, and four-body clusters is also reflected in the pair correlation functions: In g_{+-} the large contact value (see inset in Fig. 5) expresses the strong tendency of the ions to associate. The emergence of a peak near $r = 3\sigma$ (cf. Fig. 5) indicates formation of chainlike clusters. This is compatible with the development in $g_{++} = g_{--}$ (with decreasing temperature) of a strong peak at $r = 2\sigma$ which results from the increasing probability for the ions to form, at least, linear triplets

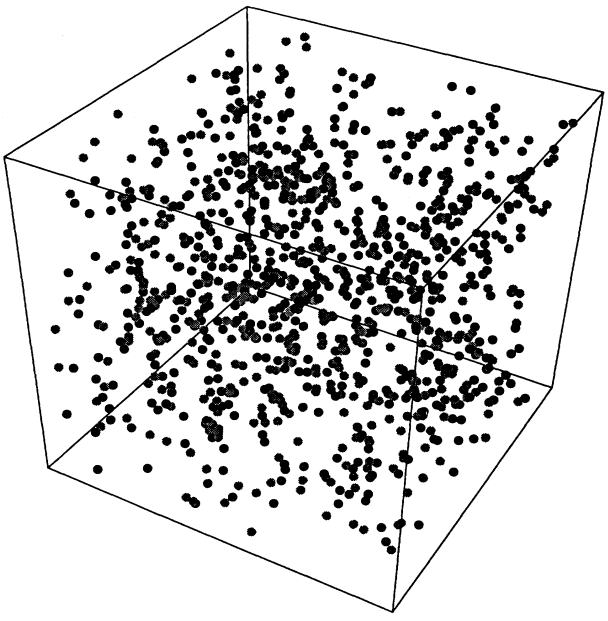

FIG. 1. Snapshot of a configuration of 512 positive and 512 negative ions in a cubic box of side 46σ with periodic boundary conditions at $\rho^* = 0.01$ and $\beta^* = 4$. The positive and negative ions are represented by black and gray dots, respectively.

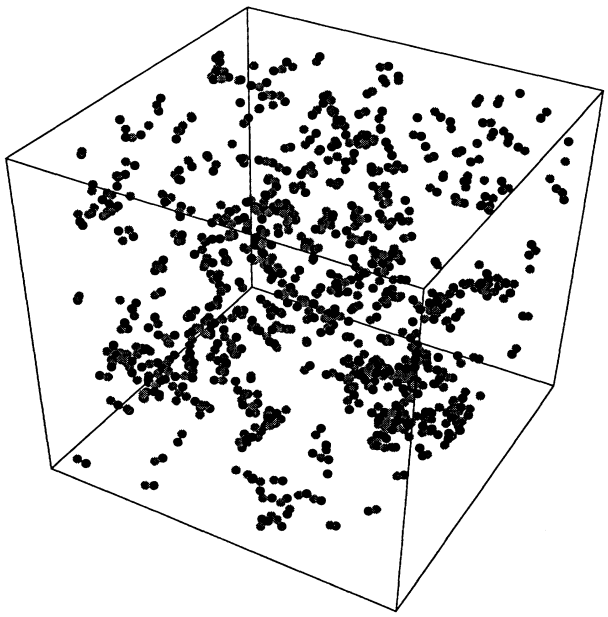

FIG. 3. Same as Fig. 1 but for $\beta^* = 15$.

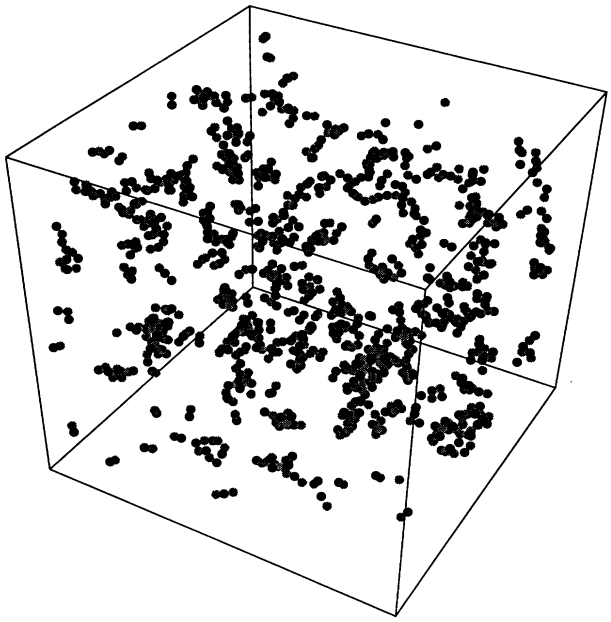

FIG. 4. Same as Fig. 1 but for $\beta^* = 18$.

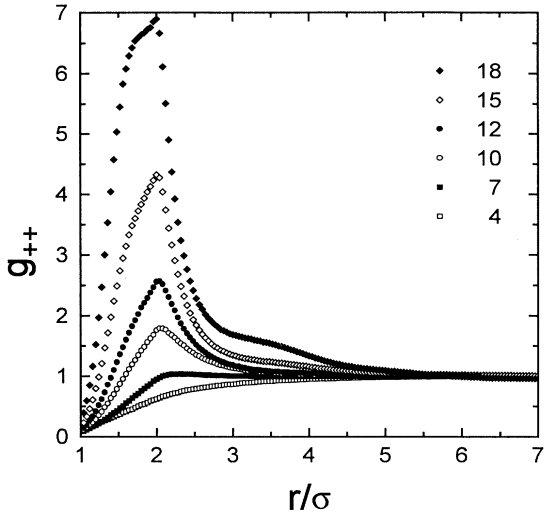

FIG. 6. Variation with temperature of the pair distribution function for like ions. The results shown are average values for g_{++} and g_{--}.

(cf. Fig. 6).

To obtain a qualitative estimate of ion cluster distribution we have analyzed instantaneous configurations of the system separated by 1000–4000 trial moves per particle according to temperature. Following Gillan [5], a group of ions is assumed to form a cluster if the distance between each member of the group and at least one other member is less than some fixed value R_c. The variation with temperature of the fraction of particles involved in monomers, dimers, and higher order clusters is summarized in Table I for the two choices $R_c = 1.5$ and 2.0σ. Several trends are apparent. First, when the temperature decreases the number of "free" ions rapidly diminishes in favor of an increase of the number of clusters of size ≥ 3. The number of dimers first increases, but decreases when the critical temperature is approached. The number of (singly) charged clusters (of size 3, 5, etc.) initially also increases but is considerably reduced near the critical temperature; there, neutral clusters are predominant. This fact is in agreement with recent computations by Caillol [3], who observes that the vapor phase is actually a dielectric gas. Let us recall that the density studied in this paper is approximately one-third of the critical den-

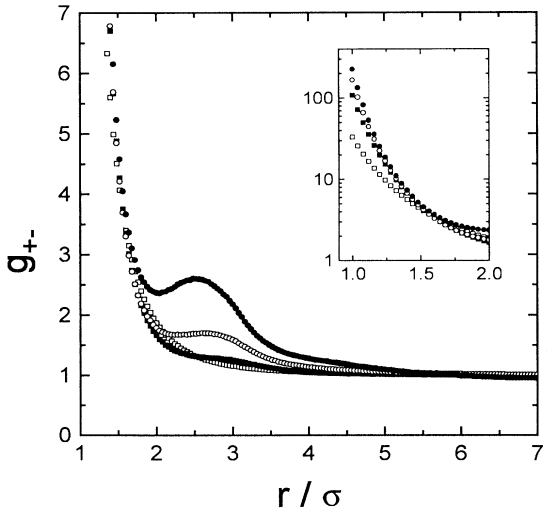

FIG. 5. Variation with temperature of the pair distribution function g_{+-} obtained from MC simulations. The symbols have the following meaning: squares $\beta^* = 7$, $\beta^* = 12$, and circles $\beta^* = 15$, $\beta^* = 18$.

TABLE I. Average fraction of particles x_n involved in clusters of size n. Variation with temperature for two values of R_c.

β^*	$R_c\sigma$	x_1	x_2	x_3	x_4	x_5	x_6	$\sum_{n\geq 7} x_n$
7	1.5	0.52	0.37	0.069	0.035			
	2.0	0.34	0.38	0.12	0.088	0.035	0.013	0.024
10	1.5	0.28	0.48	0.11	0.083	0.026	0.012	0.01
	2.0	0.15	0.42	0.18	0.13	0.050	0.083	0.077
15	1.5	0.066	0.41	0.098	0.17	0.055	0.071	0.13
	2.0	0.027	0.32	0.068	0.17	0.053	0.092	0.27
18	1.5	0.021	0.28	0.045	0.17	0.045	0.105	0.33
	2.0	0.006	0.21	0.025	0.15	0.028	0.105	0.48
20[a]	1.5	0.011	0.25	0.028	0.16	0.033	0.13	0.39
	2.0	0.003	0.20	0.014	0.17	0.021	0.12	0.47

[a]Results for 864 particles at $\rho\sigma^3 = 0.007\,27$. Averages are for 28 configurations spaced by 4000 trial moves per particle.

sity. Finally we can remark that an appreciable fraction of dimers is already present in the system at the inverse temperature $\beta^* = 7$ and that in the vicinity of the critical temperature an important fraction of ions associates into clusters involving more than six particles.

III. BRIDGE FUNCTIONS AND INTEGRAL EQUATIONS

Our next task was to determine the bridge functions $B_{\alpha\beta}(r)$ of the system from the knowledge of the pair correlation functions. This can be achieved by solving the relation

$$h_{\alpha\beta}(r_{12}) = \exp[-\beta u_{\alpha\beta}(r_{12}) + \gamma_{\alpha\beta}(r_{12}) + B_{\alpha\beta}(r_{12})] - 1 \tag{3.1}$$

coupled with the Ornstein-Zernike (OZ) equation,

$$h_{\alpha\beta}(r_{12}) - c_{\alpha\beta}(r_{12}) = \sum_{\lambda} \rho_\lambda \int c_{\alpha\lambda}(r_{13}) h_{\lambda\beta}(r_{32}) d\mathbf{r_3}, \tag{3.2}$$

where $h_{\alpha\beta} = g_{\alpha\beta} - 1$ is the total correlation function, $c_{\alpha\beta}$ the direct correlation function, $\gamma_{\alpha\beta} = h_{\alpha\beta} - c_{\alpha\beta}$, and ρ_α the density of ion species α.

For Coulombic systems it is customary to split the interaction potential into short- and long-range contributions,

$$u_{\alpha\beta} = u^{\mathrm{SR}}_{\alpha\beta}(r) + u^{\mathrm{LR}}_{\alpha\beta}(r), \tag{3.3}$$

where

$$-\beta u^{\mathrm{LR}}_{\alpha\beta}(r) = -\beta^* \frac{Z_\alpha Z_\beta}{r}(1 - e^{-\xi r}). \tag{3.4}$$

The Yukawa term in the previous equation is merely introduced for numerical purposes, to suppress the singularity at $k = 0$ in $\tilde{u}^{\mathrm{LR}}_{\alpha\beta}(k)$ [7,15]. This Yukawa parameter ξ is determined empirically to minimize errors in the transforms (see [16]) although its choice is not crucial, and in practice Eq. (3.4) represents essentially nothing but a Coulombic potential.

It is convenient to separate in a similar way the direct and total correlation functions into short- and long-range parts according to (using matrix notation)

$$\mathbf{c}^{\mathrm{SR}}(r) = \mathbf{c}(r) - \boldsymbol{\psi} \tag{3.5}$$

and

$$\mathbf{h}^{\mathrm{SR}}(r) = \mathbf{h}(r) - \mathbf{q}(r), \tag{3.6}$$

where $\psi_{\alpha\beta} = -\beta u^{\mathrm{LR}}_{\alpha\beta}(r)$ and $q_{\alpha\beta}(r)$ is a modified Debye-Hückel chain bond whose Fourier transform $\tilde{q}_{\alpha\beta}(k)$ is related to the hypervertex matrix function [7]

$$\tilde{\mathbf{v}}^{-1}(k) = \boldsymbol{\rho}^{-1}(r) - \tilde{\boldsymbol{\psi}}(k) \tag{3.7}$$

through the relations

$$\boldsymbol{\rho}\tilde{\mathbf{q}}(k)\boldsymbol{\rho} = \tilde{\mathbf{v}}(k) - \boldsymbol{\rho}. \tag{3.8}$$

The density matrix $\boldsymbol{\rho}$ has elements $\rho_{\alpha\beta} = \rho_\alpha \delta_{\alpha\beta}$.

With these definitions the OZ equation (3.2) can be rewritten in renormalized form involving only short-range functions. To do so it is convenient to introduce the functions

$$\Gamma^{\mathrm{SR}}_{\alpha\beta} = r\gamma^{\mathrm{SR}}_{\alpha\beta} = r\left[h^{\mathrm{SR}}_{\alpha\beta}(r) - c^{\mathrm{SR}}_{\alpha\beta}(r)\right], \tag{3.9}$$

$$H^{\mathrm{SR}}_{\alpha\beta}(r) = r h^{\mathrm{SR}}_{\alpha\beta}, \tag{3.10}$$

and their density-scaled Fourier transforms

$$\tilde{\Gamma}^{\mathrm{SR}}_{\alpha\beta} = k(\rho_\alpha\rho_\beta)^{1/2}\left[\tilde{h}^{\mathrm{SR}}_{\alpha\beta}(k) - \tilde{c}^{\mathrm{SR}}_{\alpha\beta}(k)\right] \tag{3.11}$$

and similarly for $\tilde{H}^{\mathrm{SR}}_{\alpha\beta}(k)$. Further writing $\tilde{V}_{\alpha\beta}(k) = (\rho_\alpha\rho_\beta)^{-1/2}\tilde{v}_{\alpha\beta}(k)$, the renormalized OZ equation takes the simple form, in Fourier space,

$$\tilde{\mathbf{\Gamma}}^{\mathrm{SR}}(k) = k^2[\tilde{\mathbf{H}}^{\mathrm{SR}}(k) + k\tilde{\mathbf{V}}(k)]^{-1} - k\tilde{\mathbf{V}}(k)^{-1} + \tilde{\mathbf{H}}^{\mathrm{SR}}(k). \tag{3.12}$$

This equation, combined with the relation (3.1), could in principle be used directly to determine the bridge functions from the known simulation results for $h_{\alpha\beta}$. In practice this way to proceed is generally somewhat awkward because even for the largest distances r calculated in the simulation (generally half the box length L), $h_{\alpha\beta}(r)$ has not yet reached its asymptotic limit. In the present calculations, although $h_{\alpha\beta}$ was calculated up to $r = 23\sigma = (L/2)$ small statistical errors in the correlation functions at large r give rise to numerical instabilities and preclude an accurate calculation of the Fourier transforms of $h_{\alpha\beta}$ (or $h^{\mathrm{SR}}_{\alpha\beta}$) at low k values. For this reason we resorted to an iterative scheme in which information on $h_{\alpha\beta}$ over a limited range of distances is combined with knowledge of the exact asymptotic behavior of the direct correlation function [13,17]. The iterative method we have used reduces to solving the renormalized OZ equation (3.2) together with the closure relation

$$\begin{aligned} h^{\mathrm{SR}}_{\alpha\beta}(r) &= h^{\mathrm{SR}}_{\alpha\beta,\mathrm{MC}}(r) \text{ if } r \le r_c, \\ c^{\mathrm{SR}}_{\alpha\beta}(r) &= -\beta u^{\mathrm{SR}}_{\alpha\beta}(r) \text{if } r > r_c, \end{aligned} \tag{3.13}$$

which is closely connected to the Duh-Haymet scheme [13]. The resulting set of nonlinear equations were solved by a method originally proposed by Labik, Malijevsky, and Vonka [18] and extended by Høye, Lomba, and Stell [7]. The reader is referred to this work for a detailed description of the method. The cutoff values r_c were chosen to be $r_c = 4.5\sigma$ for $\beta^* = 7$, $r_c = 5\sigma$ for $\beta^* = 10$, $r_c = 7.0\sigma$ for $\beta^* = 12$, $r_c = 7.0\sigma$ for $\beta^* = 15$, and $r_c = 9\sigma$ for $\beta^* = 18$.

The variation of the bridge functions with inverse temperature is shown in Fig. 7. For $r > \sigma$ the bridge functions for unlike species are always positive and decay exponentially with distance; those for like species are negative and present a discontinuity at $r = 2\sigma$, the distance at which a maximum is observed in the g_{++} and g_{--} correlation functions. Notice that these functions have essentially the same qualitative behavior that was

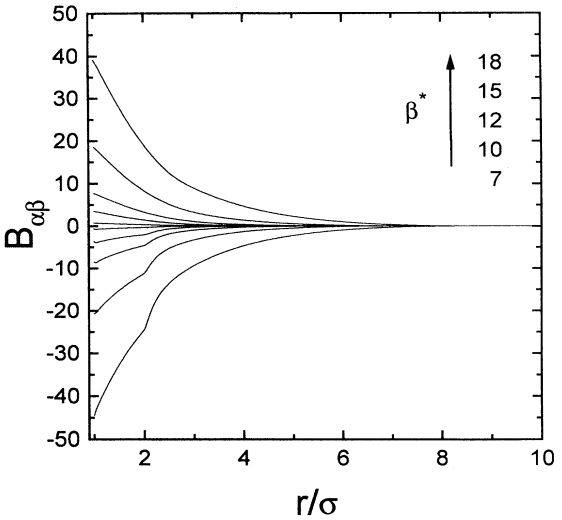

FIG. 7. Evolution of the bridge functions with inverse temperature. Positive values correspond to unlike interactions and negative to like ones.

obtained by Duh and Haymet for a model of soft-core electrolyte solutions [13]. As the temperature decreases both the range and amplitude of the bridge functions increase; however, their shape remains largely unchanged so that some temperature scaling is expected to hold. In a preliminary study we have found that bridge functions either for like or unlike interactions can be fitted to the expression

$$B_{\alpha\beta}(r) = \pm \exp[s(r)]\,(\beta^*)^{t(r)}, \tag{3.14}$$

with + and − for unlike and like interactions, respectively.

The choice of the $s(r)$ and $t(r)$ functions might be made in several ways. We have found that for unlike interactions a second degree polynomial is enough to reproduce with reasonable accuracy the "experimental" bridge function up to $r = 7\sigma$. For like interactions the functionality becomes more complex, mainly because of the singularity at $r = 2\sigma$. Nevertheless we have found that simple linear equations for $s(r)$ and $t(r)$ are able to reproduce the "experimental" data for $\sigma < r < 2\sigma$. Similarly linear functions predict the correct behavior at distances larger than 3σ. Obviously, one could resort to more elaborate fittings, but our purpose here is only to show that a simple temperature scaling holds for this system.

According to the findings of Duh and Haymet [13] and Llano-Restrepo and Chapman [12] it might be possible to find a "universal" functional for the bridge functions in terms of the short-ranged γ^{SR}. Here, we will consider the Duh-Haymet INV approximation (so called since it may be viewed as an inversion of molecular dynamic simulation data), which is particularly well suited for electrolytes [13],

$$B^{\mathrm{INV}}_{\alpha\beta} = \begin{cases} \sqrt{1+2\gamma^{\mathrm{SR}}_{\alpha\beta}} - \gamma^{\mathrm{SR}}_{\alpha\beta} - 1 & \text{if } \gamma^{\mathrm{SR}}_{\alpha\beta} \geq 0 \\ \gamma^{\mathrm{SR}}_{\alpha\beta} \exp\left(-\sqrt{-\gamma^{\mathrm{SR}}_{\alpha\beta}}\right) - \gamma^{\mathrm{SR}}_{\alpha\beta} & \text{if } \gamma^{\mathrm{SR}}_{\alpha\beta} < 0. \end{cases} \tag{3.15}$$

Notice that this functional form is strongly dependent on the decomposition of the interionic potential which in turn defines the short-range functions. According to Duh and Haymet, universality is only expected to hold if the optimized decomposition scheme is used. In this decomposition the long-range potential $\psi_{\alpha\beta}$ and the chain bond $q_{\alpha\beta}$ are related, in the case of symmetric electrolytes [13], by an OZ equation

$$\tilde{\mathbf{q}} = \tilde{\boldsymbol{\psi}} + \tilde{\boldsymbol{\psi}}\boldsymbol{\rho}\tilde{\mathbf{q}}, \tag{3.16}$$

which is coupled with the residue MSA closure. For the RPM the residue MSA closure reduces to

$$\begin{aligned} q_{\alpha\beta}(r) &= 0 \quad \text{if } r < \sigma, \\ \psi_{\alpha\beta}(r) &= -\frac{Z_\alpha Z_\beta e^2}{\epsilon r} \quad \text{if } r > \sigma. \end{aligned} \tag{3.17}$$

Along with this decomposition we have considered the simple Coulombic decomposition as explained in Sec. III. This approximation will be denoted hereafter by INV-C. Hence we will explore to what extent the INV functional form can also be used with a different choice of potential splitting.

In Fig. 8 we compare the "exact" simulation results for the bridge functions with the predictions of the INV and INV-C (Coulombic) integral equations. For $\beta^* = 7$, it is apparent that even though the INV closure underestimates the magnitude of $B(r)$ it reproduces the essential

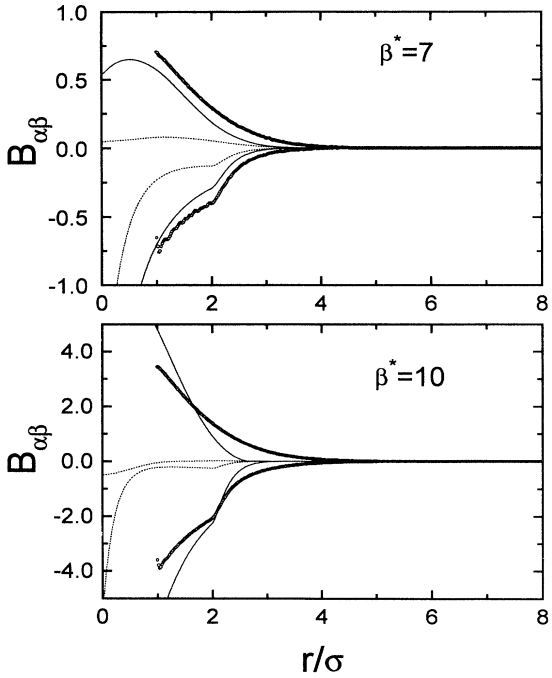

FIG. 8. "Experimental" bridge function (circles) together with results obtained using the INV (full lines) and INV-C (dotted lines) closures, for two representative temperatures.

TABLE II. Excess energy and osmotic coefficient for the RPM. Results for HNC, INV, and INV-C were obtained with 2048 grid point and a mesh $\Delta r = 0.02$.

	U/NkT				$\beta P/\rho$			
β^*	HNC	INV	INV-C	MC	HNC	INV	INV-C	MC
4.0	−0.9385	−0.9488	−0.9383	−0.945	0.7961	0.7955	0.7959	0.79
7.0	−2.1073	−2.2213	−2.1148	−2.219	0.5962	0.6066	0.5911	0.60
10.0		−4.2216	−3.4541	−3.918		0.6063	0.3778	0.43
12.0			−4.4259	−5.191			0.2328	0.40
15.0			−5.9520	−7.226			0.0054	0.32
18.0			−7.5461	−9.405			−0.2377	0.23

features of the simulation results quite well. The INV-C closure is clearly inferior, but still is able to predict the correct sign of the like and unlike bridge functions. At temperature $\beta^* = 10$, none of the closures investigated is able to predict the "exact" bridge function. The INV equation yields too large values at short distances, but still reproduces the shape of the bridge function in a qualitative way. The INV-C fails to predict the correct sign of the unlike bridge function and the magnitude of the like one is largely underestimated. Consequently, both approximations can be expected to perform poorly in the very low temperature regime.

Table II summarizes the thermodynamic properties from the INV and INV-C closures compared with the simulation results. From moderately low to high temperatures ($\beta^* < 10$) the INV approximation is the best in reproducing the thermodynamics and the structure of the system. At $\beta^* = 7$, which, for an ionic diameter $\sigma = 4.2$ Å, would correspond to a $0.1M$ aqueous 2:2 electrolyte solution at room temperature, the radial distribution functions (Figs. 9 and 10) are in very good agreement with the simulation results. More important is the prediction of the peak around 2σ for like interactions (see Fig. 9). The superiority of the INV equation is also supported by the excellent estimates of the contact values, $g_{++}(\sigma)$ and $g_{+-}(\sigma)$, at that temperature (Table III). Otherwise the INV-C closure yields essentially the same results as the HNC approximation for this range of temperatures.

At lower temperatures ($\beta^* \geq 10$) the results worsen irrespective of the closure used. The INV equation over-

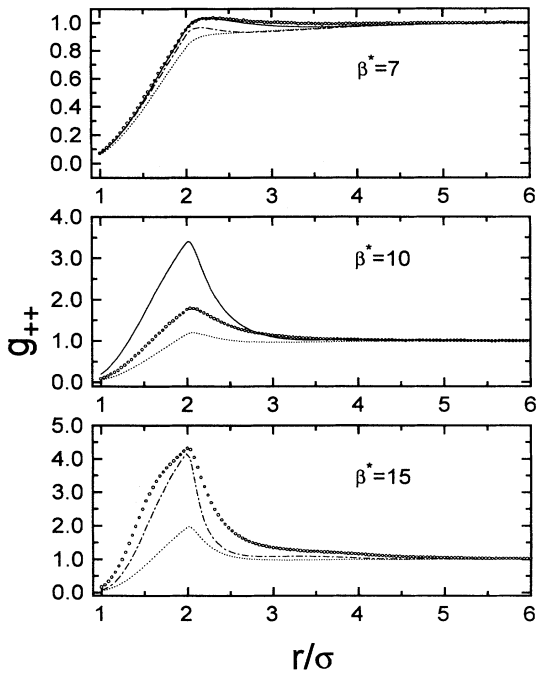

FIG. 9. Integral-equation results for the like pair correlation functions as a function of temperature. Circles represent simulation data, full lines INV approximation, and dotted lines INV-C closure. Dash-dotted lines for $\beta^* = 7.0$ correspond to HNC theory and dash-dotted lines for $\beta^* = 15$ represent the pair correlation function as predicted by the INV-C theory for $\beta^* = 23$.

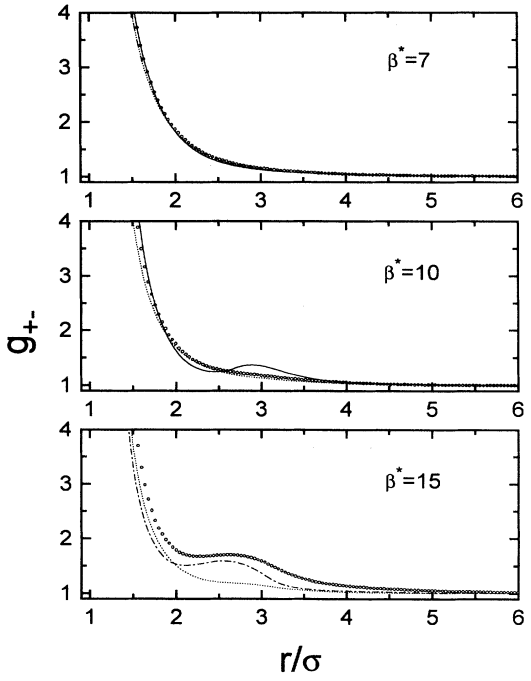

FIG. 10. Same as Fig. 9 but for g_{+-}.

TABLE III. Contact values for g_{++} and g_{+-} .

	g_{++}				g_{+-}			
β^*	HNC	INV	INV-C	MC	HNC	INV	INV-C	MC
4.0	0.111	0.111	0.111	0.11	10.29	10.56	10.27	10.1
7.0	0.073	0.069	0.061	0.07	28.45	33.07	28.21	33
10.0		0.194	0.055	0.08		96.59	50.48	71
12.0			0.052	0.10			67.57	108
15.0			0.051	0.16			94.43	165
18.0			0.053	0.24			121.95	226

estimates the energy, pressure, as well as the correlation functions (see Figs. 9 and 10). We have found that this approximation fails to converge for inverse temperatures larger than $\beta^* = 10$, whereas the INV-C has solutions for the entire range of β^* considered in this work. From inspection of Figs. 9 and 10 one can readily appreciate that the INV-C equation underestimates the fluid structure. For a given temperature the INV-C predicts a structure that would correspond to that of a system at a somewhat higher temperature. In particular, the use of an inverse temperature $\beta^* = 23$ gives a much improved representation of the MC pair correlation functions at $\beta^* = 15$. Eloquent support to this improvement is given by the development of a hump in $g_{+-}^{\mathrm{INV-C}}$ near $r \approx 2.5\sigma$ (cf. Fig. 10) having its origin in four-particle association. This result suggests that a simple reparametrization of the INV-C approximation could lead to an improved agreement with the MC results. Besides, from the above results one might speculate on the use of a hybrid between the two decomposition schemes, i.e., Coulombic and optimized, as a way to improve the theoretical estimates in these harsh thermodynamic conditions.

Finally, in Fig. 11 we show $\gamma_{\alpha\beta}(r)$ as a function of temperature. For every β^*, γ_{++} presents a singularity at $r = 2\sigma$ characteristic of the formation of linear triplets. This cusp at 2σ (which also appears in B_{++}) is a mathematical consequence of the nearly Dirac δ-like behavior of g_{+-} close to the core. From Eq. (3.2) one sees that

$$\gamma_{++}(r_{12}) = \rho_- \int h_{+-}(r_{13}) h_{-+}(r_{32}) d\mathbf{r}_3 + \cdots$$

and a convolution of two $\delta(r-\sigma)$ functions gives rise to a step function with the singularity at 2σ, $H(r-2\sigma)$. Since the h_{+-} does not really diverge at the core, the step function singularity is smoothed into a cusp.

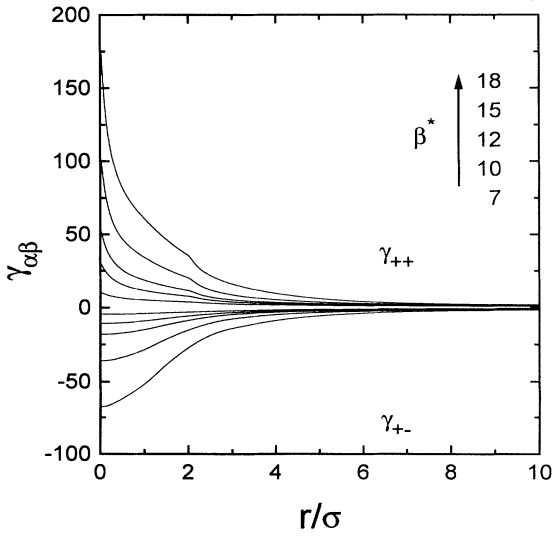

FIG. 11. Evolution of the $\gamma_{\alpha\beta}$ function when approaching the critical region.

IV. SUMMARY

We have used MC simulations to determine the cluster population and the bridge functions of the RPM near the critical region. The cluster analysis was based on configurations separated by 1000–4000 trial moves per particle. Over such a "time" span appreciable migration of the ions and evolution of the clusters is established. This is in accordance with previous studies of model electrolyte solutions [19] (our RPM model with $\beta^* = 7$ is roughly equivalent to a $0.1M$ aqueous solution of a 2:2 electrolyte at room temperature). Clusters are not stable entities but dissociate and reform. In particular we have verified that in configurations separated by periods of the order of 100 trial moves per particle a given ion had a different environment and generally belonged to a different cluster. This finding gives support to the adequacy of the simple sampling scheme used despite the rather strong interactions between the ions. It does not seem necessary, at least for the temperature domain here considered, to invoke more complicated sampling schemes involving, for instance, displacement and rotation of full clusters.

When the critical temperature is approached an increasingly large fraction of ions is found to partake in the formation of neutral clusters of size greater than 4 and even 6 at the expense of dimers and charged clusters ("free" ions, triplets, etc.) in agreement with recent theoretical analysis [20,21]. Nonetheless, it can be seen that even at the lowest temperature considered, a small number of conducting entities remains present in the system.

A second goal of the present study was the determination of the bridge functions. This function is shown to have a rather simple shape depending smoothly on temperature. For the like species the net effect of the

bridge function results is an increased repulsion between particles, whereas for the unlike ions it amounts to an enhancement of the attractive interactions. A recently proposed approximation which expresses the bridge function in terms of γ^{SR} only has been solved using two decomposition schemes of the interionic potential, namely, optimized (INV) and Coulombic (INV-C) splittings. It is found that the INV approximation predicts excellent results for $\beta^* < 10$ but at lower temperatures it overestimates the structure of the system. Otherwise the INV-C yields essentially the same results as the HNC approximation for low β^*. Contrary to the HNC and INV closures, the INV-C is fully convergent for the entire set of temperatures considered in this work, although it underestimates the structure of the system. We obtain fair evidence, however, that a simple reparametrization of the bridge function or perhaps a hybrid decomposition scheme of the interionic potential could remedy much of this deficiency.

ACKNOWLEDGMENTS

This work was partially supported by Grants No. PB90-0233 and PB91-0110 furnished by the Dirección General de Investigación Científica y Tecnológica of Spain. Fruitful correspondence with A.D.J. Haymet is acknowledged. One of us (J.J.W.) would like to thank D. Levesque and J.M. Caillol for interesting discussions. The Monte Carlo calculations were performed on the parallel computer C98 of Institut du Développment et des Ressources en Informatique Scientifique (IDRIS), Orsay (France).

[1] M.E. Fisher, J. Stat. Phys. **75**, 1 (1994).
[2] (a) A.Z. Panagiotopoulos, Fluid Phase Equilibria **92**, 313 (1994); (b) G. Orkoulas and A.Z. Panagiotopoulos, J. Chem. Phys. **101**, 1452 (1994).
[3] J.M. Caillol, J. Chem. Phys. **100**, 2161 (1994).
[4] J.P. Valleau, L.K. Cohen, and D.N. Card, J. Chem. Phys. **72**, 5942 (1980).
[5] M.J. Gillan, Mol. Phys. **49**, 421 (1983).
[6] M.E. Fisher and Y. Levin, Phys. Rev. Lett. **71**, 3826 (1993).
[7] J.S. Høye, E. Lomba, and G. Stell, Mol. Phys. **75**, 1217 (1992).
[8] M. Medina-Noyola, J. Chem. Phys. **81**, 5059 (1984).
[9] E. González-Tovar, M. Lozada-Cassou, L. Mier-y-Terán, and M. Medina-Noyola, J. Chem. Phys. **95**, 6784 (1991).
[10] F. Bresme, E. Lomba, and J.L.F. Abascal (unpublished); detailed results are available upon request.
[11] M. Llano-Restrepo and W.G. Chapman, J. Chem. Phys. **97**, 2046 (1992).
[12] M. Llano-Restrepo and W.G. Chapman, J. Chem. Phys. **100**, 5139 (1994).
[13] D.M. Duh and A.D.J. Haymet, J. Chem. Phys. **97**, 7716 (1992).
[14] See, e.g., M.P. Allen and D.J. Tildesley, *Computer Simulation of Liquids* (Clarendon, Oxford, 1989).
[15] J.F. Springer, M.A. Pokrant, and F.A. Stevens, J. Chem. Phys. **58**, 4863 (1973).
[16] E. Lomba and J.S. Høye, Comput. Phys. Commun. **69**, 420 (1992).
[17] L. Verlet, Phys. Rev. **165**, 201 (1968).
[18] S. Labik, A. Malijevsky, and P. Vonka, Mol. Phys. **56**, 709 (1985).
[19] J.L.F. Abascal and P. Turq, Chem. Phys. **153**, 79 (1991); J.L.F. Abascal, F. Bresme, and P. Turq, Mol. Phys. **81**, 143 (1994).
[20] K.S. Pitzer and D.R. Schreiber, Mol. Phys. **60**, 1067 (1987).
[21] D. Laria, H.R. Corti, and R. Fernández-Prini, J. Chem. Soc. Faraday Trans. **86**, 1051 (1990).